Atomic population distribution of excited states in He electrodeless discharge lamp

Zhiming Tao (陶智明)[1,2], Yanfei Wang (王彦飞)[1], Shengnan Zhang (张盛楠)[1], Dongying Wang (王东颖)[1], Yelong Hong (洪叶龙)[1], Wei Zhuang (庄 伟)[1*], and Jingbiao Chen (陈景标)[1]

[1]*State Key Laboratory of Advanced Optical Communication System and Network, Institute of Quantum Electronics, School of Electronics Engineering and Computer Science, Peking University, Beijing 100871, China*

[2]*Department of Physics, Bijie University, Bijie 551700, China*

[*]*Corresponding author: wzhuang@pku.edu.cn*

Received April 27, 2013; accepted August 14, 2013; posted online September 29, 2013

Population ratios between excited states are measured to build the excited state Faraday anomalous dispersion optical filter (ESFADOF). We calculate these values between the excited states according to the spontaneous transition probabilities using rate equations and the measured intensities of fluorescence spectral lines of He atoms in an electrodeless discharge lamp in the visible spectral region from 350 to 730 nm. The electrodeless discharge lamp with populations in excited states can be used to realize the frequency stabilization reference of the laser frequency standard. This lamp can also build ESFADOFs for submarine communication application in the blue-green wavelength to simplify the system without the use of a pump laser.

OCIS codes: 020.0020, 020.1335, 300.6210.
doi: 10.3788/COL201311.100202.

The electrodeless discharge lamp containing atoms and ions is applied in various scientific devices such as radiation and absorption spectrometers, spectrometer-goniometers, frequency standard[1,2], and magnetometers[3]. Discharge lamps have been used for optical pumping[4] instead of lasers in these devices because these lamps can yield fluorescence with a stable frequency and higher signal-to-noise ratios[5]. The fluorescence of an electrodeless discharge lamp can be used as a pumping light source for an active optical clock[6,7], a multi-threshold second-order phase transition[8], and a Faraday anomalous dispersion optical filter[9]. The lamp can also be used in specific applications such as the frequency stabilization reference of the laser frequency standard[10−12] and the excited state Faraday anomalous dispersion optical filter (ESFADOF) for submarine and underwater communication in the blue-green wavelength. Various characteristics of the discharge lamp of He atoms have been investigated over the years. For example, theoretical and experimental investigations of the pulsed excitation of low-pressure He and Xe glow discharges have been reported[13]. AC-driven, low-pressure He-Xe lamp discharges have also been studied experimentally[14]. The radiative characteristic of a high-frequency eletrodeless He lamp has been calculated using the model developed[15]. Furthermore, spectral lines of a He eletrodeless discharge lamp at 1083 nm have been significantly applied in atomic magnetometers[16,17].

Our group recently used Rb electrodeless discharge lamps to build ESFADOFs[18,19]. We focused on investigating the population distribution of excited states in the visible spectral region of the He electrodeless discharge lamp to build an ESFADOF for submarine communication in the blue-green wavelengths of 447, 471, 492, 501, and 504 nm.

The bulb in the lamp is a cylindrical glass cell with a length of 4.5 cm and a diameter of 3.5 cm (Fig. 1). It contains natural He atoms at 5 torr and is supplied with 32–MHz radio frequency (RF) power. Thus, the bulb is excited by the field of an external RF coil of 2 turns, and the excited vapor is a mixture of He atoms and He ions. The USB2000+ spectrometer (Ocean Optics Company, USA) with a resolution of 1.5 nm is used to measure the fluorescence spectra. The full-width at half-maximum (FWHM) of observed spectral lines is limited by the resolution bandwidth of the spectrometer. The true FWHM of the spectral lines should be near the Doppler broadening of 0.5 MHz. When the RF voltage is set at 7 V, its current is then set at 0.5 A.

The energies of the electrons and ions inside the lamp with He atoms increase after they are accelerated by the high-frequency electric field[1]. These high-energy electrons and ions collide with the He atoms, producing more electrons and ions. They also excite the He atoms to a higher level. When the He atoms transit from a high level to a low level by spontaneous radiation, they release fluorescence. At this point, the spectra of He atoms appear.

The lamp works between 3 and 10 V of RF voltages. Regardless of the operating voltage of the lamp, the population ratio between the excited states of He atoms is almost constant. For simplicity, we did not consider the working voltage when the intensity of the fluorescence spectral lines of He atoms was measured.

Fig. 1. Experimental scheme of a He electrodeless discharge lamp for spectrum research.

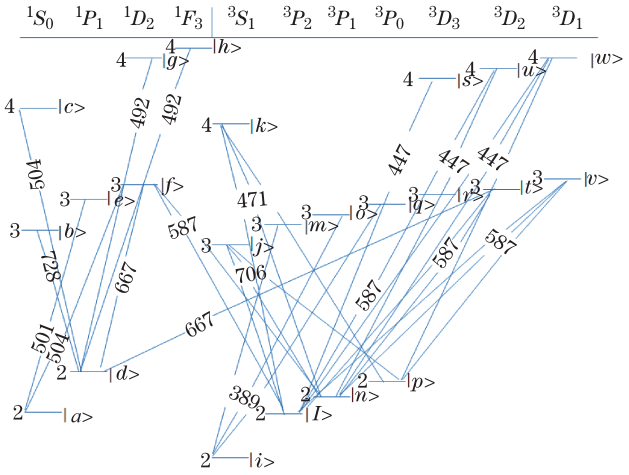

Fig. 2. Energy level diagram of He atoms transitions.

Figure 1 shows the block diagram of our experimental arrangement, and Fig. 2 shows the energy diagram of the transitions related to the spectral signal.

When the distance of the spectrometer from the He lamp is set appropriately, the relative intensities of the spectral lines of He atoms can be detected (Fig. 3). The result is calibrated by the spectral response curve of the spectrometer. The relative intensities in arbitrary units of 389, 447, 471, 492, 501, 504, 587, 667, 706, and 728 nm are 21 634, 12 923, 10 274, 12 425, 54 901, 9 786, 64 329, 39 078, 42 712, and 15 876, respectively. Several small signals in Fig. 3 are assigned to weak spectral lines that are not considered in this letter. The intensity of the different spectral lines of He atoms vary widely, of which 587 nm is the strongest, 501 nm ranks second, and 504 nm is the weakest in our measurements.

Table 1. Spectral Signal Relative Intensities, Wavelengths, Spontaneous Transition Probabilities, Configurations, Terms, and Total Angular Momentum Quantum Number

Intensity (a. u.)	Wavelength (nm)	$A_{\mu\eta} \times (10^6 s^{-1})$	Configurations	Terms	$J_I - J_k$
21634	388.86046	A_{qi}=9.4746	1*s*2*s*-1*s*3*p*	^3S-^3P	1-0
	388.86455	A_{oi}=9.4746	1*s*2*s*-1*s*3*p*	^3S-^3P	1-1
	388.86489	A_{mi}=9.4746	1*s*2*s*-1*s*3*p*	^3S-^3P	1-2
12923	447.14703	A_{wl}=0.6827	1*s*2*p*-1*s*4*d*	^3P-^3D	2-1
	447.14740	A_{ul}= 6.1440	1*s*2*p*-1*s*4*d*	^3P-^3D	2-2
	447.14743	A_{sl}= 24.579	1*s*2*p*-1*s*4*d*	^3P-^3D	2-3
	447.14856	A_{wn}= 10.241	1*s*2*p*-1*s*4*d*	^3P-^3D	1-1
	447.14893	A_{un}= 18.432	1*s*2*p*-1*s*4*d*	^3P-^3D	1-2
	447.16832	A_{wp}= 13.655	1*s*2*p*-1*s*4*d*	^3P-^3D	0-1
10274	471.31391	A_{kl} =5.2894	1*s*2*p*-1*s*4*s*	^3P-^3S	2-1
	471.31561	A_{kn} =3.1736	1*s*2*p*-1*s*4*s*	^3P-^3S	1-1
	471.33756	A_{kp} =1.0579	1*s*2*p*-1*s*4*s*	^3P-^3S	0-1
12425	492.06127	A_{hd} =6.219*10^{-5}	1*s*2*p*-1*s*4*f*	^1P-^1F	1-3
	492.19310	A_{gd} =19.863	1*s*2*p*-1*s*4*d*	^1P-^1D	1-2
54901	501.56779	A_{ea} =13.372	1*s*2*s*-1*s*3*p*	^1S-^1P	0-1
9786	504.20874	A_{fa} =1.022*10^{-4}	1*s*2*s*-1*s*3*d*	^1S-^1D	0-2
	504.77385	A_{cd} =6.7712	1*s*2*p*-1*s*4*s*	^1P-^1S	1-0
64329	587.44338	A_{fl} =4.310* 10^{-3}	1*s*2*p*-1*s*3*d*	^3P-^1D	2-2
	587.44602	A_{fn}=1.232* 10^{-2}	1*s*2*p*-1*s*3*d*	^3P-^1D	1-2
	587.55986	A_{vl} =1.9641	1*s*2*p*-1*s*3*d*	^3P-^3D	2-1
	587.56139	A_{tl}=17.673	1*s*2*p*-1*s*3*d*	^3P-^3D	2-2
	587.56148	A_{rl} =70.708	1*s*2*p*-1*s*3*d*	^3P-^3D	2-3
	587.56250	A_{vn} =29.462	1*s*2*p*-1*s*3*d*	^3P-^3D	1-1
	587.56403	A_{tn} =53.019	1*s*2*p*-1*s*3*d*	^3P-^3D	1–2
	587.59662	A_{vp} =39.282	1*s*2*p*-1*s*3*d*	^3P-^3D	0-1
39078	667.81517	A_{fd} =63.705	1*s*2*p*-1*s*3*d*	^1P–^1D	1–2
	667.96768	A_{td} =1.51* 10^{-2}	1*s*2*p*-1*s*3*d*	^1P-^3D	1-2
42712	706.51771	A_{jl} =15.474	1*s*2*p*-1*s*3*s*	^3P-^3S	2-1
	706.52153	A_{jn}=9.2844	1*s*2*p*-1*s*3*s*	^3P-^3S	1-1
	706.57086	A_{jp} =3.0948	1*s*2*p*-1*s*3*s*	^3P-^3S	0-1
15876	728.13507	A_{bd} =18.299	1*s*2*p*-1*s*3*s*	^1P-^1S	1-0

The intensity (p) of the transition signal between two energy levels can be expressed as $p_\lambda = n_\mu A_{\mu\eta} h\nu_\lambda$, where λ is the transition wavelength, n_μ is the atomic density in the level numbered μ ($\mu = a, b, c\ldots$), $A_{\mu\eta}$ is the spontaneous transition probability between the μ and η energy levels, ν is the transition frequency, and h is Plank constant. The transition signal intensity studied can be clearly expressed with rate equations as

$$p_{389} = n_m A_{mi} h\nu_{389} + n_o A_{oi} h\nu_{389} + n_q A_{qi} h\nu_{389}, \quad (1)$$

$$p_{447} = n_s A_{sl} h\nu_{447} + n_u A_{ul} h\nu_{447} + n_w A_{wl} h\nu_{447} + n_u A_{un} h\nu_{447} + n_w A_{wn} h\nu_{447} + n_w A_{wp} h\nu_{447}, \quad (2)$$

$$p_{471} = n_k A_{kl} h\nu_{471} + n_k A_{kn} h\nu_{471} + n_k A_{kp} h\nu_{471}, \quad (3)$$

$$p_{492} = n_g A_{gd} h\nu_{492} + n_h A_{hd} h\nu_{492}, \quad (4)$$

$$p_{501} = n_e A_{ea} h\nu_{501}, \quad (5)$$

$$p_{504} = n_f A_{fa} h\nu_{504} + n_c A_{cd} h\nu_{504}, \quad (6)$$

$$p_{587} = n_f A_{fl} h\nu_{587} + n_f A_{fn} h\nu_{587} + n_r A_{rl} h\nu_{587} + n_t A_{tl} h\nu_{587} + n_t A_{tn} h\nu_{587} + n_v A_{vl} h\nu_{587} + n_v A_{vn} h\nu_{587} + n_v A_{vp} h\nu_{587}, \quad (7)$$

$$p_{667} = n_f A_{fd} h\nu_{667} + n_t A_{td} h\nu_{667}, \quad (8)$$

$$p_{706} = n_j A_{jl} h\nu_{706} + n_j A_{jn} h\nu_{706} + n_j A_{jp} h\nu_{706}, \quad (9)$$

$$p_{728} = n_b A_{bd} h\nu_{728}. \quad (10)$$

The spontaneous transition probabilities, $A_{\mu\eta}$, and the wavelengths involved in the calculation are listed in Table 1[20] Data in columns 1–6 are spectral signal intensities, wavelengths, spontaneous transition probabilities, configurations, terms, and total angular momentum quantum number, respectively.

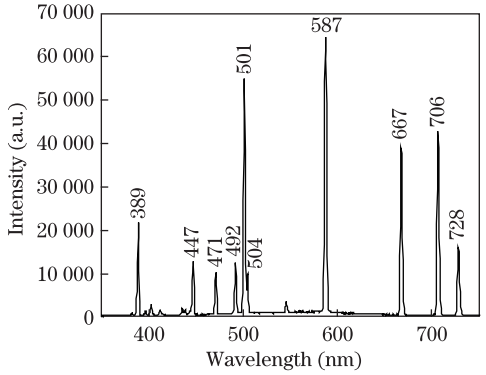

Fig. 3. Intensities of spectral lines of He atoms.

Table 2. Calculation Results of n_μ/n_e

n_μ/n_e	Value
$(n_m + n_o + n_q)/n_e$	0.431
$(n_s + n_u + n_w)/n_e$	0.114
n_k/n_e	0.247
n_g/n_e	0.150
n_c/n_e	0.354
$(n_r + n_t + n_v)/n_e$	0.260
n_f/n_e	0.199
n_j/n_e	0.527
n_b/n_e	0.307

From Eqs. (1)–(10), the 501-nm transition has only one spectral line corresponding to the transition, $1s3p^1P_1 \rightarrow 1s2s^1S_0$. Given that the population in the $|e>$ energy level is the maximum, the value of n_e is used as the benchmark to calculate the results of n_μ/n_e.

The calculated results of n_μ/n_e are shown in Table 2. As shown in Table 2 and Fig. 2, the population in the $|e>$ energy level that corresponds to the 501-nm transition reaches a maximum value in all transitions. The population in the $|j>$ energy level that corresponds to the 706-nm transition ranks second. The populations in the other energy levels are also very large. The electrodeless discharge lamp with populations in excited states can be used to realize the frequency stabilization reference of the laser frequency standard[10]. ESFADOF can also be used for submarine communication in the blue-green wavelength to simplify the system without the use of a pump laser[18,19].

In conclusion, population ratios between the excited states according to the spontaneous transition probabilities with rate equations and the measured intensities of fluorescence spectral lines of He atoms in electrodeless discharge lamp in the visible spectral region from 350 to 730 nm are calculated. Sufficient populations in the excited states are found when the lamp is lit[18−21]. The electrodeless discharge lamp with populations in excited states can be used to realize the frequency stabilization reference of the laser frequency standard[10]. ESFADOF can also be used for submarine communication in the blue-green wavelength to simplify the system without the use of a pump laser[9,18].

This work was supported by the National Natural Science Foundation of China under Grant Nos. 10874009 and 11074011. The authors wish to thank Dr. Wei Gong for his beneficial discussion and direction of this research.

References

1. Y. Wang, J. Fu, and T. Dong, *Principle of Quantum Frequency Standard* (in Chinese)(Science Press, Beijing, 1986) p. 391.
2. F. Riehle, *Frequency Standards* (Wiley VCH, Weinheim, 2004) p. 248.
3. E. B. Alexandrov and V. A. Bonch-Bruevich, Opt. Eng. **31,** 711 (1992).
4. J. C. Camparo and C. M. Klimcak, J. Appl. Phys. **99,** 083306 (2006).
5. Z. Yang, Y. Li, H. Wang, Q. Lu, and X. Xu, Chin. Opt. Lett. **9,** 061401 (2011).
6. S. Huo, Z. Zhang, Z. Wu, H. Zheng, T. Liu, X. Xue, J. Song, and Y. Zhang, Chin. Opt. Lett. **9,** 121902 (2011).
7. J. C. Camparo, J. Opt. Soc. Am. B. **15,** 1177 (1998).
8. Y. Wang, Chin. Sci. Bull. **54,** 347 (2009).
9. J. Chen, Chin. Sci. Bull. **54,** 348 (2009).
10. W. Zhuang, D. Yu, and Z. Liu, Chin. Sci. Bull. **56,** 3812 (2011).
11. H. Guo, A. Dang, Y. Han, S. Gao, Y. Cao, and B. Luo, Chin. Sci. Bull. **55,** 527 (2010).
12. X. Miao, L. Yin, W. Zhuang, and J. Chen, Rev. Sci. Instrum. **82,** 086106 (2011).
13. R. Bussiahn, S. Gortchakov, H. Lange, and D. Loffhagen, J. Phys. D Appl. Phys. **39,** 66 (2006).
14. R. Bussiahn, S. Gortchakov, H. Lange, D. Loffhagen, and

D. Uhrlandt, J. Phys. D Appl. Phys. **40,** 3882 (2007).
15. N. V. Denisova and A. Skudra, Opt. Spectrosc. **95,** 884 (2003).
16. M. K. Plante and D. L. MacFarlane, Phys. Rev. A **82,** 013837 (2010).
17. N. Tateiwa, Y. Haga, Z. Fisk, and Y. Onuki, Rev. Sci. Instrum. **82,** 053906 (2011).
18. Q. Sun, W. Zhuang, Z. Liu, and J. Chen, Opt. Lett. **36,** 4611 (2011).
19. Q. Sun, Y. Hong, W. Zhuang, and J. Chen, Appl. Phys. Lett. **101,** 211102 (2012).
20. http: //physics. nist. gov/cgi-bin/ASD/linesl/.
21. Q. Sun, X. Miao, R. Sheng, and J. Chen, Chin. Phys. B. **21,** 033201 (2012).